Organic Geochemistry 65 (2013) 83–93

Contents lists available at ScienceDirect

Organic Geochemistry

journal homepage: www.elsevier.com/locate/orggeochem

Differential degradation of intact polar and core glycerol dialkyl glycerol tetraether lipids upon post-depositional oxidation

Sabine K. Lengger [a,*], Mariska Kraaij [a], Rik Tjallingii [b], Marianne Baas [a], Jan-Berend Stuut [b,c], Ellen C. Hopmans [a], Jaap S. Sinninghe Damsté [a], Stefan Schouten [a]

[a] Department of Marine Organic Biogeochemistry, Royal NIOZ Netherlands Institute for Sea Research, P.O. Box 59, 1790AB Den Burg, Texel, The Netherlands
[b] Department of Marine Geology, Royal NIOZ Netherlands Institute for Sea Research, Texel, The Netherlands
[c] MARUM-Center for Marine Environmental Sciences, MARUM – Center for Marine Environmental Sciences, University of Bremen, Leobener Str., D-28359 Bremen, Germany

ARTICLE INFO

Article history:
Received 4 March 2013
Received in revised form 11 July 2013
Accepted 3 October 2013
Available online 10 October 2013

ABSTRACT

Archaeal and bacterial glycerol dialkyl glycerol tetraether lipids (GDGTs) are used in various proxies, such as TEX_{86} and the BIT index. In living organism, they contain polar head groups (intact polar lipids – IPLs). IPL GDGTs have also been detected in ancient marine sediments and it is unclear whether or not they are fossil entities or are part of living cells. In order to determine the extent of degradation of IPL GDGTs over geological timescales, we analyzed turbidite deposits, which had been partly reoxidized for several kyr after deposition on the Madeira Abyssal Plain. Analysis of core lipid (CL) and IPL-derived GDGTs showed a reduction in concentration by two orders of magnitude upon post-depositional oxidation, while IPL GDGTs with a mono- or dihexose head group decreased by 2–3 orders of magnitude. The BIT index for CL- and IPL-derived GDGTs increased substantially upon oxidation from 0.1 to up to 0.5. Together with changing MBT/CBT values, this indicates preferential preservation of soil-derived branched GDGTs over marine isoprenoid GDGTs, combined with in situ production of branched GDGTs in the sediment. The TEX_{86} value for IPL-derived GDGTs decreased by 0.07 upon oxidation, while that of CL GDGTs showed no significant change. Isolation of IPLs revealed that the TEX_{86} value for monohexose GDGTs was 0.55, while the that for dihexose GDGTs was substantially higher, 0.70. Thus, the decrease in TEX_{86} for IPL-derived GDGTs was in agreement with the dominance of monohexose GDGTs in the oxidized turbidite, probably caused by a combination of in situ production as well as selective preservation of terrestrial isoprenoid GDGTs. Due to the low amount of IPL GDGTs vs. CL GDGTs, the impact of IPL degradation on CL-based TEX_{86} paleotemperature estimates was negligible.

1. Introduction

TEX_{86} (tetraether index of tetraethers consisting of 86 carbons) and BIT (branched and isoprenoid tetraether) index are proxies based on archaeal and bacterial glycerol dialkyl glycerol tetraether lipids (GDGTs). The BIT index is based on the relative amounts of the abundant, mainly marine, isoprenoid GDGT crenarchaeol (Fig. 1a) and branched GDGTs (brGDGTs), which are produced mainly in terrigenous environments (Fig. 1b). It is therefore used to quantify the relative amount of soil contribution to the organic matter (OM) in marine sediments (Hopmans et al., 2004). Proxies based on brGDGTs are the CBT index, based on the relative amount of cyclopentane moieties in brGDGTs, which correlates with pH, and the MBT/CBT proxy, based on the degree of methylation and cyclization of brGDGTs, which correlates with mean annual air temperature (MAT; Weijers et al., 2007; Peterse et al., 2012). The lipids used for TEX_{86} are isoprenoid GDGTs (iGDGTs) containing different amounts of cyclopentane or cyclohexane moieties (Fig. 1a) and which are produced in marine environments by archaea, in particular the Thaumarchaeota, formerly classified as Marine Group I Crenarchaeota (Brochier-Armanet et al., 2008; Spang et al., 2010). TEX_{86} from marine suspended matter and surface sediments has shown to be related to sea surface temperature (Schouten et al., 2002; Wuchter et al., 2005, 2006a). It has been calibrated globally in order to enable quantification of past sea surface temperature (SST; Kim et al., 2008, 2010).

In living archaea, iGDGTs occur with polar head groups, such as hexoses and phosphate groups, bound to the hydroxyl group at the sn-1 position of the glycerol moiety by glycosidic or ester bonds, respectively (Fig. 1c; e.g. Koga and Morii, 2005; Schouten et al., 2008; Albers and Meyer, 2011). Upon cell death, most of these intact polar lipids (IPLs) are transformed to core lipids (CLs) via hydrolysis of the polar head groups (White et al., 1979). This supposedly rapid loss of functional groups resulted in their use as suitable markers for living cells, in contrast to the core lipids, which

* Corresponding author. Present address: Petroleum and Environmental Geochemistry Group, Biogeochemistry Research Centre, Plymouth University, Drake Circus, Plymouth, Devon PL4 8AA, UK. Tel.: +44 17525584556.
E-mail address: sabine.lengger@plymouth.ac.uk (S.K. Lengger).

0146-6380/$ - see front matter © 2013 Elsevier Ltd. All rights reserved.
http://dx.doi.org/10.1016/j.orggeochem.2013.10.004

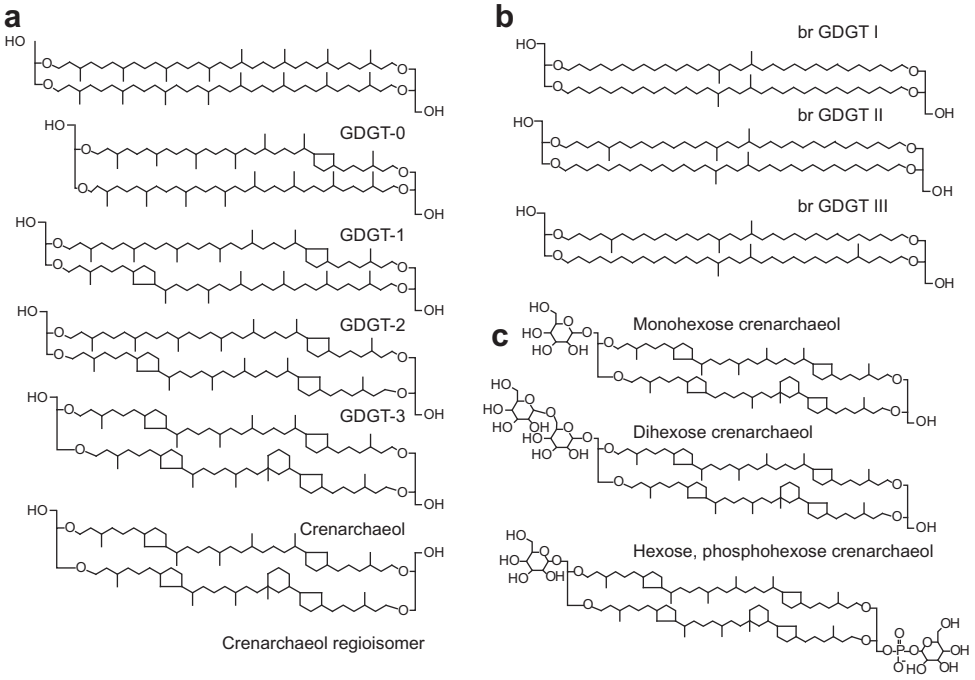

Fig. 1. Structures of GDGTs. Isoprenoid CL GDGTs (a), branched CL GDGTs (b) and measured IPL crenarchaeol species (c).

can be preserved over geological timescales of millions of years (e.g. Kuypers et al., 2001; Jenkyns et al., 2012).

Considerable amounts of IPL GDGTs (10–10,000 ng g^{-1} sediment) have been found in shallow to deeply buried marine sediments [0.7 to 121 m below sea floor (mbsf)], which suggests the presence of a large number of living archaeal cells (Biddle et al., 2006; Lipp et al., 2008; Lipp and Hinrichs, 2009). However, the degradation rate of certain IPL GDGTs might potentially be lower than that of bacterial phospholipids, resulting in preservation of IPL GDGTs over geological time (Harvey et al., 1986; Schouten et al., 2010; Logemann et al., 2011; Lengger et al., 2012b). Indeed, Lengger et al. (2012b) found evidence for substantial degradation of the hexose, phosphohexose (HPH) crenarchaeol (for structures see Fig. 1c) within 1–2 kyr but not for monohexose (MH) and dihexose (DH) crenarchaeol. The reason for this may be that the phosphoester bond is less stable than the glycosidic bond. As most IPL GDGTs in deeply buried sediments are comprised of glycolipids rather than phospholipids, it is possible that these lipids are simply preserved more efficiently. Furthermore, degradation experiments by Logemann et al. (2011) showed that archaeal IPL GDGTs were barely degraded in sediments over a time period of 100 days, in contrast to bacterial and eukaryotic ester lipids that become decayed within weeks. Finally, recent experiments conducted by Xie et al. (2013) over a slightly longer timescale (300 d) also suggest a low degradation rate for glycosidic ether lipids. However, how degradation rates for IPL GDGTs differ from each other is not clear, nor is the impact of oxygen exposure time, especially over geological timescales.

The degradation of CL GDGTs has been investigated in more detail by focusing on comparing anoxic and oxic depositional settings. Sediments deposited under anoxic and oxic conditions were compared using sediment cores from the Arabian Sea, which exhibited concentration differences in the GDGTs (Sinninghe Damsté et al., 2002). Although the GDGT concentration changed between these anoxic and oxic sediments, the GDGT distributions and TEX_{86} values remained unaffected (Schouten et al., 2004). This study is supported by data from Kim et al. (2009), who showed that TEX_{86} values remained unaffected after organic-rich sediments, deposited under anoxic conditions, were exposed for 1 yr to oxygenated water. However, turbidite deposits of the Madeira Abyssal Plain (MAP) that cover the last 140 kyr did indicate a substantial effect of 10 kyr post-depositional oxidation on GDGT concentration (Huguet et al., 2008, 2009).

The sedimentary sequence of the MAP is characterized by massive distal turbidite deposits (Buckley and Cranston, 1988). They comprise organic-rich sediments deposited in an O_2 minimum zone at the shelf, and are completely mixed by turbiditic transport before deposition at the oxygenated MAP. These mixed and organic-rich sediments are oxidized by an oxidation front that moves slowly downward after deposition, referred to as the process of diagenetic burn-down (De Lange, 1992). This process of oxidation causes a decrease in lipid concentration that can reach up to two orders of magnitude (Cowie et al., 1995, 1998; Prahl et al., 1997; Hoefs et al., 2002). The substantial decrease in the concentration of all GDGTs across similar oxidation fronts of the MAP, as reported by Huguet et al. (2008), occurred in combination with preferential degradation of iGDGT over brGDGT compounds. Consequently, this preferential degradation resulted in a substantial increase in the BIT index across these fronts. The preferential preservation of brGDGTs was attributed to the difference in matrix protection or to the lower initial reactivity of soil OM transported over longer distances before deposition (Middelburg, 1989; Huguet et al., 2008). Oxidation of the CL GDGTs can also cause either an increase or a decrease in TEX_{86} values, which was related to enhanced preservation of terrestrial iGDGTs of variable composition (Huguet et al., 2009).

For IPL GDGTs, however, the effect of post-depositional oxidation has not been examined. Previous studies, which observed changes in IPL GDGT distributions in sediments, have almost exclusively attributed this to the incorporation of a signal from in situ produced IPL GDGTs (Lipp et al., 2008; Lipp and Hinrichs, 2009; Schubotz et al., 2009; Liu et al., 2011). In situ production was suggested by Hoefs et al. (2002), who found apparently high preservation efficiency of C_{16} and C_{18} fatty acids, which was attributed, in part, to bacterial in situ production in the sediment. However, evidence has emerged that the in situ production of IPL GDGTs may

effectively be quite low (Takano et al., 2010; Lin et al., 2012; Xie et al., 2013), except for settings with high activity such as a sulfate-methane transition zone, and is thus unlikely to cause a substantial change in IPL GDGT distributions.

Here, we investigate the long term (ca. 10 kyr) effect of post-depositional oxygen exposure on the distribution of IPL GDGTs and CL GDGTs in the f-turbidite of the MAP (Buckley and Cranston, 1988). We analyzed CL GDGT and IPL GDGT concentrations and the respective TEX_{86}, BIT and MBT/CBT values for a fresh sediment core from the unoxidized f-turbidite, the overlying oxidized hemipelagic sediments and the overlying unoxidized e-turbidite. The stratigraphic borders between these depositional units were obtained independently using a combination of grain size analysis and statistical clustering of the inorganic sediment composition. The results were used to examine the sources and degradation of IPL GDGTs and their effect on GDGT based indices.

2. Material and methods

2.1. Sampling

The core (MAP-1) was taken during cruise JCR209 onboard the R/V James Clark Ross in September 2007 using a piston corer. Location was the MAP in the eastern North Atlantic at 31°26.8′N 024°48.8′W in the proximity of well-studied turbidite deposits (De Lange, 1992; Cowie et al., 1995, 1998; Prahl et al., 1997; Hoefs et al., 2002; Huguet et al., 2008, 2009). The f-turbidite is a > 140 kyr old, ca. 4 m thick, OM rich turbidite at ca. 10–12 mbsf, with 40–50 cm oxidized sediment on top of the unoxidized turbidite, equivalent to ca. 10 kyr of oxidation (Buckley and Cranston, 1988). It was labeled "f" (Weaver and Kuijpers, 1983; Weaver et al., 1989) for being one turbidite deposit in a series of such deposits of varying OM content. Based on these studies, the f-turbidite was expected at ca. 10 m core depth at our coring location. The recovered core (ca. 12 m) was cut in half and inspected visually for differences in sediment color and type. The sections most likely containing the f-turbidite were sub-sampled at 2–20 cm resolution from 9 to 12 m on board the ship. Samples were stored in geochemical bags and kept frozen at - 20 °C until analysis.

2.2. Particle size analysis

Samples (29) from 9 to 12 m were analyzed for particle size distribution, after isolation of the terrigenous fraction (cf. McGregor et al., 2009). For removal of organic carbon (OC) and $CaCO_3$, ca. 500 mg sediment were boiled in 10 ml 35% H_2O_2 until reaction ceased and excess H_2O_2 degraded to H_2O and O_2, then in 10 ml of 10% HCl for 1 min to remove the $CaCO_3$ and diluted 10 × (twice each time) with H_2O to neutral pH. Immediately prior to particle size analysis, the OM-free, and $CaCO_3$-free sediment was boiled with 300 mg $Na_4P_2O_7{\cdot}10H_2O$ to ensure particle disaggregation. The particle size of the non-soluble fraction was analyzed in degassed H_2O using a Beckmann-Coulter Laser Particle Sizer LS230, which measures particle size from 0.04–2000 μm and describes 116 size classes.

2.3. Total OC (TOC) content

Freeze-dried and homogenized samples were analyzed for TOC content. An aliquot of freeze-dried sediment was decalcified (overnight, 2 N HCl) and washed with bidistilled H_2O, which was removed by freeze drying. TOC was measured with a Flash EA 1112 Series (Thermo Scientific) analyzer coupled via a Conflo II interface to a Finnigan Delta^{plus} mass spectrometer. It is reported as the average of duplicate measurements, with a standard deviation ⩽ 0.2% of TOC.

2.4. X-ray fluorescence (XRF) core scanning and statistical analysis

The inorganic composition of the sediments was analyzed using a Avaatech XRF core scanner (Tjallingii et al., 2007), which uses energy-dispersive fluorescence radiation to measure composition as element intensity in counts s^{-1} in a non-destructive way. Loosely packed samples were prepared by pressing ca. 4 g freeze dried powder into a sample cup without additional binder and covering them with SPEXCerti Ultralene® foil. Measurements were conducted at 10 and 30 kV using a count time of 10 s, which acquired intensity data for 13 elements (Al, Ca, Cl, Fe, K, Mn, S, Si, Ti, Br, Rb, Sr, Zr). The 30 kV run was performed in combination with a Pd thin filter to suppress the background radiation that originates from the primary X-ray source and increases at higher source power. The element intensities provided by XRF core scanning represent the count rate of each individual element after integration of the measurement time. Element intensities measured on dry powder material are primarily related to element concentration (Tjallingii et al., 2007). However, matrix absorption effects and enhancement effects might potentially bias element intensity data, whereas log ratios of element intensities are linearly related to log ratios of element concentrations (Weltje and Tjallingii, 2008). Therefore, log ratios of element intensities provide the most easily interpretable signals in terms of relative changes in composition.

Objective identification of the main stratigraphic boundaries in the core was accomplished using a statistical clustering approach for the total data set acquired from XRF core scanning. To provide statistically significant stratigraphical boundaries, a centered log ratio transformation was applied to describe the variance in all measured 13 elements. The transformation has been shown to convert compositional data to a statistically meaningful co-variance matrix free of closed-sum effects (Aitchison, 1981). Centered log ratios (CLRs) are expressed as $CLR_i = \ln[I_i/g]$, where I is the intensity of an individual element *i*, and *g* the geometric mean of all 13 element intensities. Subsequently, a principal component analysis of the CLR matrix indicated that the first two principal components explained 78.8% of the total variance. The distribution of the principal component scores (Fig. 2a) clearly resolved several subpopulations. Four statistically meaningful clusters were identified by K mean clustering of the CLR matrix, which is a standard routine in the open source software PAST.

2.5. Lipid extraction and IPL/CL separation

Lipids were extracted with a modified Bligh–Dyer extraction method (Bligh and Dyer, 1959) as described by Lengger et al. (2012a). One aliquot of the extract was used directly for analysis of IPL GDGTs via liquid chromatography-electrospray ionization-tandem mass spectrometry HPLC–ESI–MS^2 and another for separation of IPL GDGTs from CL GDGTs over a SiO_2 column according to Pitcher et al. (2009) except that the first eluent was adjusted to hexane/EtOAc 1:2 (v/v) to minimize carryover. To both the IPL and the CL fraction, 0.1 μg internal GDGT C_{46} standard was added (cf. Huguet et al., 2006). The IPL fraction was hydrolyzed under reflux in 5% methanolic HCl to give the IPL derived GDGTs, which were extracted 3 × from the aqueous phase with dichloromethane (DCM; cf. Pitcher et al., 2009). CL- and IPL-derived GDGT concentrations were analyzed via HPLC-atmospheric chemical ionization (APCI)-MS and peak areas were normalized to the internal standard. The standard was corrected for the difference in relative response to crenarchaeol using a C_{46}/crenarchaeol 1:1 (wt./wt.) mixture. IPL fractions were tested for carryover of CL GDGTs by analysis of a small amount before hydrolysis by HPLC-APCI-MS. Carryover was typically < 2% of the CL and < 20% of the IPL-derived GDGTs. IPL-derived amounts represent the concentrations measured after hydrolysis and corrected for the carryover.

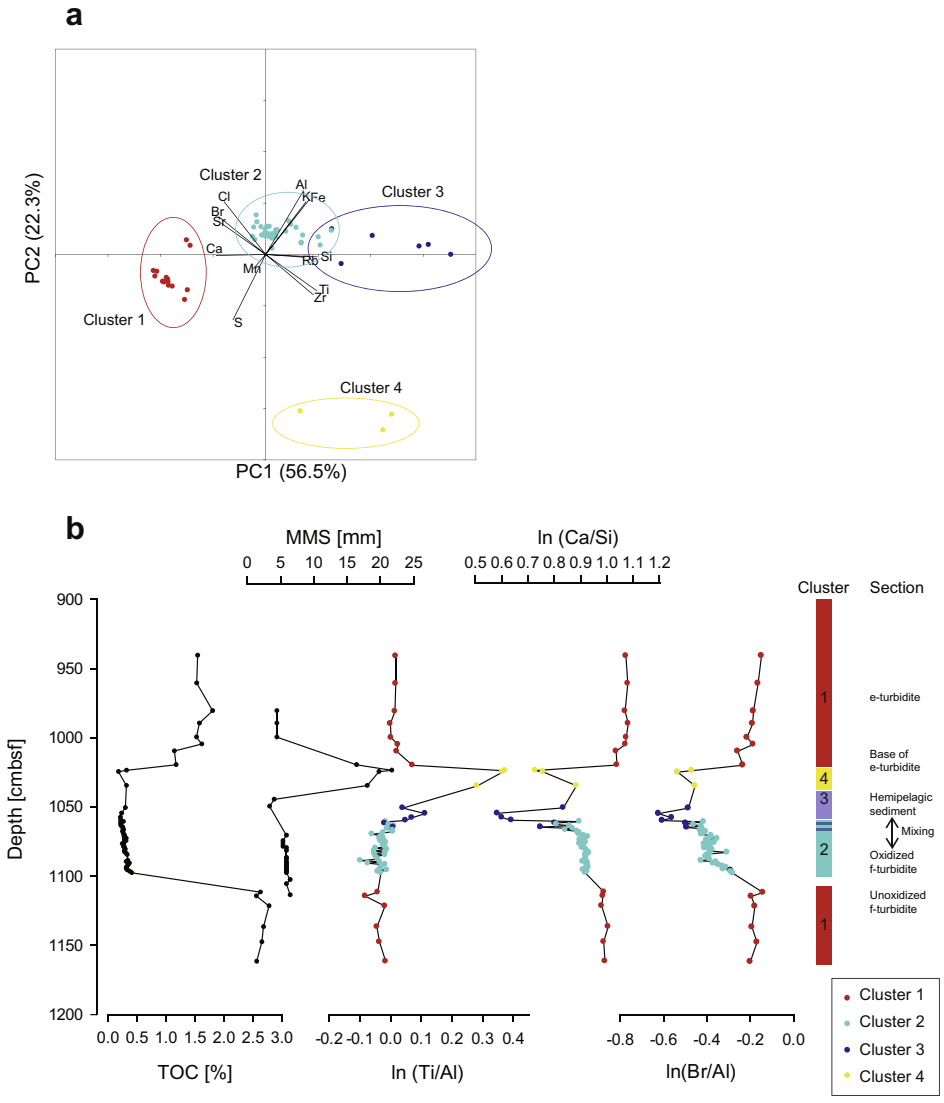

Fig. 2. Results of PCA and clustering analysis of XRF core scanning data. (a) Bi-plot of PC1, PC2 and individual chemical elements. (b) Depth profiles of TOC, mean modal grain size (MMS) and ln(Ca/Si), ln (Ti/Al) and ln(Br/Ti).

2.6. HPLC-APCI-MS and HPLC–ESI-MS^2

CL- and IPL-derived GDGTs were analyzed as described by Schouten et al. (2007). TEX_{86} values and the corresponding SST estimates were calculated according to the TEX_{86}^H calibration of Kim et al. (2010) and typically show a standard deviation < 0.02 TEX_{86}. CBT and MBT values and derived temperature values were determined according to Weijers et al. (2007). HPLC–ESI–MS^2 in selected reaction monitoring (SRM) mode as described by Pitcher et al. (2011a), using conditions modified from Sturt et al. (2004), was used to analyze selected IPL GDGTs. Those monitored were MH crenarchaeol, DH crenarchaeol and HPH crenarchaeol. The latter was detected just above detection limit and was therefore not quantified. Due to a lack of standards, the results are reported as arbitrary area units (aaus). Signal stability was monitored using a lipid extract of *Candidatus* Nitrososphaera gargensis (Pitcher et al., 2010) that was injected every 8 runs. Quantification of IPL concentration was done based on results from preparative HPLC. In order to determine concentration in ng per gram sediment dry wt., ng (g sed dw)$^{-1}$, the average MS response peak area for the unoxidized sediment (1111.5 cmbsf, 1136.5 cmbsf, 1147.5 cmbsf, 1161.5 cmbsf) was divided by the actual concentration of crenarchaeol obtained after hydrolysis of the semi-preparative HPLC fraction of the individual crenarchaeol IPL (see below), which gave a correction factor (8.0×10^{-5} ng aau^{-1} for MH crenarchaeol and 1.3×10^{-5} ng aau^{-1} for DH crenarchaeol), allowing us to determine the concentration from the SRM peak areas. All concentrations given are as (g sed dw)$^{-1}$.

2.7. Semi-preparative HPLC

To isolate IPL GDGTs, semi-preparative HPLC was used as described by Schouten et al. (2008) and Lengger et al. (2012b). A mixture of the extracts from four samples (1111.5 cmbsf, 1136.5 cmbsf, 1147.5 cmbsf and 1161.5 cmbsf) of 0.7 g sediment each of the unoxidized f-turbidite, was separated using an Agilent (San Jose, CA, USA) 1100 series LC instrument with an Inertsil diol column (250 × 10 mm; 5 µm; Alltech Associates Inc., Deerfield, IL) at 3 ml min^{-1} and identical mobile phase and gradient as for intact polar lipid LC–MS^2 analysis (see above and Pitcher et al., 2011a). Fractions (3 ml) were collected and measured by way of flow injection analysis using ESI–MS^2 in SRM mode under the same conditions as for analytical SRM, monitoring the same transitions. The solvent was 60% A [hexane/isopropanol/HCO_2H/14.8 M NH_3 aq. (79/20/0.12/0.04, v/v/v/v)] and 40% B [isopropanol/water/HCO_2H/14.8 M NH_3 aq. (88/10/0.12/0.04, v/v/v/v)]. The fractions contain-

ing MH GDGTs were combined, as well as the DH GDGTs. No other IPL-GDGTs were present in detectable amount. Fractions were acid-hydrolyzed and the MH- and DH-derived GDGTs analyzed via HPLC-APCI-MS as described above.

3. Results and discussion

3.1. Sedimentology and stratigraphy

The stratigraphy of the core section between 1162 and 905 cmbsf was established using TOC, grain size distribution of the lithogenic sediment fraction and bulk inorganic sediment composition obtained from XRF core scanning (Fig. 2b). Over this interval, TOC concentration varied from 0.3% to 2.6%. A high concentration (avg. 2.6 ± 0.08%) was found between 1162 and 1111.5 cmbsf, above which values dropped abruptly to ca. 0.3%. The TOC concentration remained low between 1100 and 1024.5 cmbsf, but increased again to 1.1–1.8% above this interval (Fig. 2b). This pattern of TOC concentration is typical for the transition between two turbidites that, based on their stratigraphic depth, corresponds with the transition from the unoxidized and oxidized f- and the unoxidized e-turbidite, respectively (cf. Weaver and Kuijpers, 1983; Buckley and Cranston, 1988; Weaver et al., 1989). Based on the TOC profile the boundary between the oxidized and unoxidized part of the f-turbidite was set at ca. 1105 cmbsf.

Grain size distribution with a uniform mean modal size (MMS) of 5.8 μm was found up to 1070.5 cmbsf, followed by a slight decrease to 3.3–4.0 μm between 1070.5 and 1044.5 cmbsf (Fig. 2b). The core interval between 1034.5 and 1019.5 cmbsf revealed a substantial increase in MMS to 16–20 μm, which decreased again to 4.4 μm at and above 999.5 cmbsf. The strong MMS increase between 1034.5 and 1019.5 cmbsf corresponded with a similar increase in bulk sediment ln(Ti/Al) ratio. Off NW Africa, the joint variability in grain size and sediment composition reveals that the Ti/Al ratio corresponds with relative variation in the lithogenic silt and clay fractions (Bloemsma et al., 2012).

Statistical clustering of the XRF data (Fig. 2a) revealed four stratigraphic boundaries that related to variation in the lithogenic grain size, as well as change in sediment composition. The first stratigraphic boundary was indicated by a strong reduction in TOC and a simultaneous drop in ln(Br/Al) values, which is indicative for the boundary between the unoxidized and the oxidized part of the f-turbidite. However, it is unclear if the compositional changes at this boundary are related to grain size variation due to the lack of grain size data for this interval. The stratigraphic boundary between clusters 2 and 3 resulted mainly from a relative increase in siliciclastic sediments, as indicated by reduced ln(Ca/Si) values, whereas TOC and MMS remained constant. Low TOC concentration at the oxidized part of the f-turbidite results from degradation of OM and is also characteristic of hemipelagic sediments. The boundary between the oxidized upper part of the f-turbidite and hemi-pelagic sediments is commonly revealed as a bioturbated mixing interval several cm thick (Buckley and Cranston, 1988). Mixing over this transition was also reflected in the alternation between cluster 2 and 3 around this boundary (Fig. 2b). The base of the e-turbidite was clearly identified from the abrupt increase in MMS and ln(Ti/Al) values at 1044.5 cmbsf and marks the boundary between clusters 3 and 4 (Fig. 2b). Turbidites are characterized by a coarse grained and well sorted base overlain by an upward fining sequence that follow a sequence of depositional changes during and after these events (Bouma, 1962). Fine grained sediments with higher TOC concentration overlie these relatively coarse grained sediments. These sediments represent the unoxidized e-turbidite and are indicated by an identical sediment composition to cluster 1. Since we wanted to investigate the impact of post-depositional oxidation on IPL degradation and TEX_{86}, we analyzed IPL GDGTs and CL GDGTs from 1162 to 1076 cmbsf, representing the unoxidized and oxidized f-turbidite without interference from hemipelagic sedimentation.

3.2. Oxic degradation of brGDGTs: CLs and IPLs

BrGDGTs were present in low concentration relative to iGDGTs, as commonly observed in open marine sediments (Schouten et al., 2013 and references therein). In the oxidized part of the turbidite deposit, the concentration decreased by two orders of magnitude, i.e. from 87 to 3.8, and 26 to 0.9 ng (g sed dw)$^{-1}$ for the CL fraction and the IPL fraction, respectively (Fig. 3a and b; Table 1). The changes occurred gradually (Fig. 3a and b). Based on concentration, we could calculate the apparent (i.e. assuming no in situ production) preservation efficiency for individual GDGTs, i.e. the concentration of a GDGT in the oxidized part of the turbidite (avg. 1076.5 to 1095.5 cmbsf) as a proportion (%) of the average concentration in the unoxidized part (avg. of 1111.5 to 1161.5 cmbsf; cf. Sinninghe Damsté et al., 2002; Hoefs et al., 2002). The apparent preservation efficiency was 4.4% for CL-derived and 3.5% for IPL-derived brGDGTs, less than reported by Huguet et al. (2008), who found 8% of the CL brGDGTs preserved in the sediment which had been subjected longest to oxic conditions. For comparison, the apparent preservation efficiency of TOC was 10% (20% in the f-turbidite of Huguet et al., 2008). This suggests that the oxidized interval analyzed by Huguet et al. had been less exposed to oxic conditions, although the interval of oxidized sediment examined here was of the same thickness (20 cm).

In general, brGDGTs are assumed to derive from terrigenous sources, mainly soil OM (e.g. Hopmans et al., 2004; Weijers et al., 2009; Peterse et al., 2011; Smith et al., 2012). However, they have been shown to be also produced in situ in small amount in marine sediments (Peterse et al., 2009; Zhu et al., 2011). Indeed, their presence in the IPL-derived fraction could indicate that they are, in part, produced in situ. For the turbidite deposits, this could mean that the brGDGTs were either produced in situ in the original shelf sediments or that they were produced after deposition of the turbidites on the abyssal plain. In order to obtain clues about their origin, we determined the MBT and CBT values for the CL GDGTs. Unfortunately, this was not possible for the IPL fraction due to the low abundance and limited amount of material. Interestingly, the CBT value from CL brGDGTs in the unoxidized section was relatively low (0.01–0.03; Fig. 3c), corresponding to a relatively high pH of 8.8, using the Weijers et al. (2007) calibration. Since the pH of African soils is typically much lower (< 8; Weijers et al., 2007), this suggests that these brGDGTs are produced in situ in marine sediments (cf. Peterse et al., 2009). The MBT values for the unoxidized turbidite were 0.28–0.29 (Fig. 3d), and the MAT calculated from MBT/CBT using the Weijers et al. (2007) calibration was relatively low, i.e. 8.2–8.4 °C (Fig. 3e). Since MAT values on the African continent are much higher (> ca. 10 °C), this is also consistent with a dominant origin of these CL brGDGTs from in situ production in the sediment rather than from soil OM. These in situ produced brGDGTs could already be produced at the continental shelf, before the sediment is transported to the abyssal plain and deposited as a turbidite, or after deposition. This latter possibility is, however, not consistent with the significant changes in the distribution of the brGDGTs. In the oxidized turbidite deposits, the brGDGT distribution gradually changed to give a higher CBT value (0.3, corresponding to pH 7.9) and a higher MBT value (0.35–0.45), resulting in higher calculated MAT (9–13 °C). In combination with the observed substantial decrease in the concentration of the brGDGTs (Fig. 3a and b), this suggests that the CBT and MBT values changed due to preferential preservation of brGDGTs from a different provenance., i.e. soil OM (cf. Huguet et al., 2008). These terrigenous

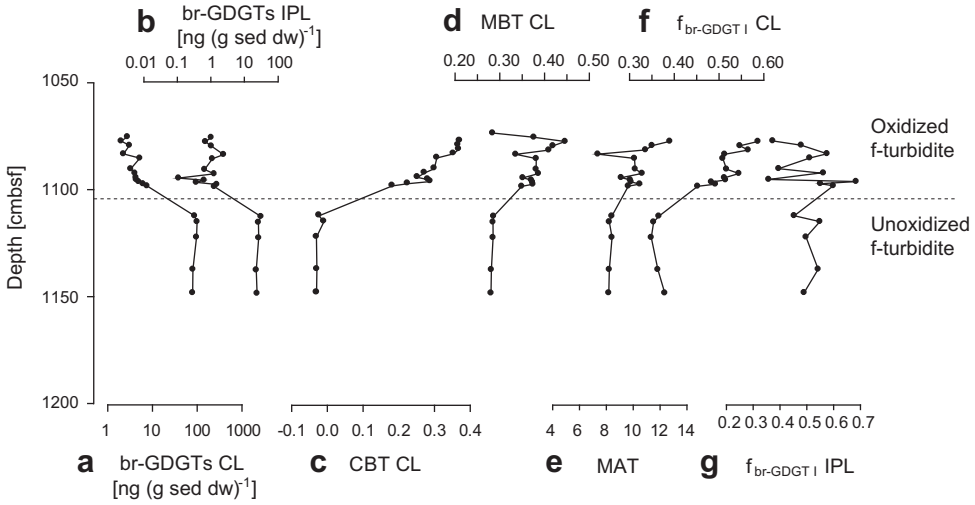

Fig. 3. GDGT-concentrations and GDGT-derived ratios in the f-turbidite. CL- and IPL-derived brGDGT concentration (a, b, note log scale), CBT values (c), MBT values for CL GDGTs (d), MAT calculated for CL GDGTs from MBT/CBT (e), and $f_{brGDGT\ I}$ for the CL- (f) and IPL-derived brGDGTs (g).

Table 1
Average concentration in oxidized and unoxidized part of the turbidite and apparent preservation efficiency (concentration in the oxidized section divided by concentration in unoxidized section) for the CL- and IPL-derived GDGTs (concentration for CL is in ng per g sediment dry wt.).

	brGDGTs	GDGT-0	Crenarchaeol	Minor iGDGTs
CL				
Unoxidized	87.3 ± 9.0	4360 ± 230	5540 ± 320	1621 ± 90
Oxidized	3.83 ± 1.1	13.5 ± 3.3	13.7 ± 4.0	4.13 ± 1.2
IPL-derived				
Unoxidized	26.3 ± 3.4	110 ± 27	111 ± 20	99 ± 8.7
Oxidized	0.9 ± 0.7	2.4 ± 1.0	0.6 ± 0.6	0.5 ± 0.1
IPL-derived (% of total)				
Unoxidized	23	2.5	2.0	5.8
Oxidized	19	15	3.8	11
Apparent preservation efficiency (%)				
CL	4.4	0.31	0.25	0.25
IPL	3.5	2.2	0.49	0.52

GDGTs would likely be characterized by higher CBT and MBT values, reflecting a lower pH and higher MAT, as they would be derived from subtropical northwestern African soils. Therefore, the compositional differences in CL brGDGTs between the oxidized and unoxidized part of the f-turbidite can be explained by selective preservation of terrestrial vs. marine brGDGTs. Such an enhanced preservation could be due to better protection by the inorganic soil matrix in which they are embedded (Keil et al., 1994). Terrigenous OM, having endured long distance transport, is exposed to oxic degradation over a longer time than marine material and the remaining compounds are therefore relatively well protected from degradation. This was defined by Middelburg (1989) as a lower "initial reactivity" of the terrigenous OM.

Intriguingly, the IPL-derived brGDGTs were preserved to an almost similar degree as the CL-derived brGDGTs (Table 1). This seems irreconcilable with the idea that IPL GDGTs are more labile than CL GDGTs and would suggest a similar degree of preservation for IPL-derived GDGTs as for CL GDGTs. To investigate the provenance of these GDGTs, we also determined their distribution. However, as the concentration of many of the brGDGTs was too low for accurate determination of MBT and CBT values, we used the fractional abundance of the dominant GDGTs, i.e. brGDGTs I, II and III. The fraction of brGDGT I, $f_{brGDGT\ I}$ (i.e. the concentration of brGDGT I divided by the sum of brGDGTs I, II and III; for structures see Fig. 3b), was used as an indicator of distributional change. The $f_{brGDGT\ I}$ of the IPL-derived GDGTs showed no substantial change between the unoxidized and oxidized part, in contrast to the CL GDGTs (Fig. 3e). This, together with the high apparent preservation efficiency, suggests that most of the IPL brGDGTs, particularly those in the oxidized part, had been produced in situ. The fact that, in the CL GDGT fraction, a strong change in distribution was observed, suggests that these in situ produced IPL brGDGTs, forming < 5% of the CL GDGTs, did not have a major impact on CL GDGT distribution. This may be due to the relatively low production rate of these compounds in the marine environment (i.e. BIT values in open marine sediments are nearly always < 0.1; Schouten et al., 2013) and possibly the relatively rapid degradation of in situ produced IPL GDGTs vs. fossil GDGTs (cf. Lengger et al., 2012b).

3.3. Oxic degradation of iGDGTs, CLs and IPLs

In the unoxidized section of the f-turbidite, CL iGDGT concentration was between 4 and 6 μg (g sed dw)$^{-1}$ for the most abundant GDGTs, i.e. GDGT-0 and crenarchaeol, with lower amount of the minor iGDGTs used for determination of TEX_{86}, i.e. their summed concentration was 1.5–1.7 μg (g sed dw)$^{-1}$ (Fig. 4a; Table 1). IPL-derived GDGTs had a much lower concentration, from 0.1–0.2 μg (g sed dw)$^{-1}$ for GDGT-0 and crenarchaeol and 0.5 and 1.0 μg (g sed dw)$^{-1}$ for the minor iGDGTs (Fig. 4b; Table 1). In the oxidized part, the concentration decreased by two orders of magnitude, i.e. to 13 ng (g sed dw)$^{-1}$ for CL GDGT-0 and crenarchaeol, and 4 ng (g sed dw)$^{-1}$ for the sum of the minor iGDGTs (Fig. 4). The concentration of IPL-derived iGDGTs was also reduced in the oxidized section by at least two orders of magnitude. Concentration in the oxidized part was 2.4 and 0.6 ng (g sed dw)$^{-1}$ for crenarchaeol and GDGT-0, and 0.5 and 1.0 ng (g sed dw)$^{-1}$ for the minor iGDGTs. These changes initially occurred abruptly and then more gradually over the first 10 cm of the oxidized part of the turbidite (Fig. 4).

The apparent preservation efficiency for CL iGDGTs was 0.25–0.31% and 0.49–2.2% for IPL-derived iGDGTs, substantially lower than for TOC and brGDGTs (Table 1). These results are similar to those reported by Huguet et al. (2008) for the f-turbidite, i.e. the branched CL GDGTs were preserved more efficiently than the CL iGDGTs (0.2% for crenarchaeol vs. 7% for brGDGTs in Huguet et al., 2008). This is likely due to the greater terrigenous contribution to brGDGTs than to iGDGTs. Surprisingly, the apparent preservation efficiency was slightly higher for IPL-derived iGDGTs than for CL iGDGTs, though still substantially lower than for TOC and with a considerable standard deviation (Table 1). Most likely, the same explanation as for IPL-derived brGDGTs could be applied

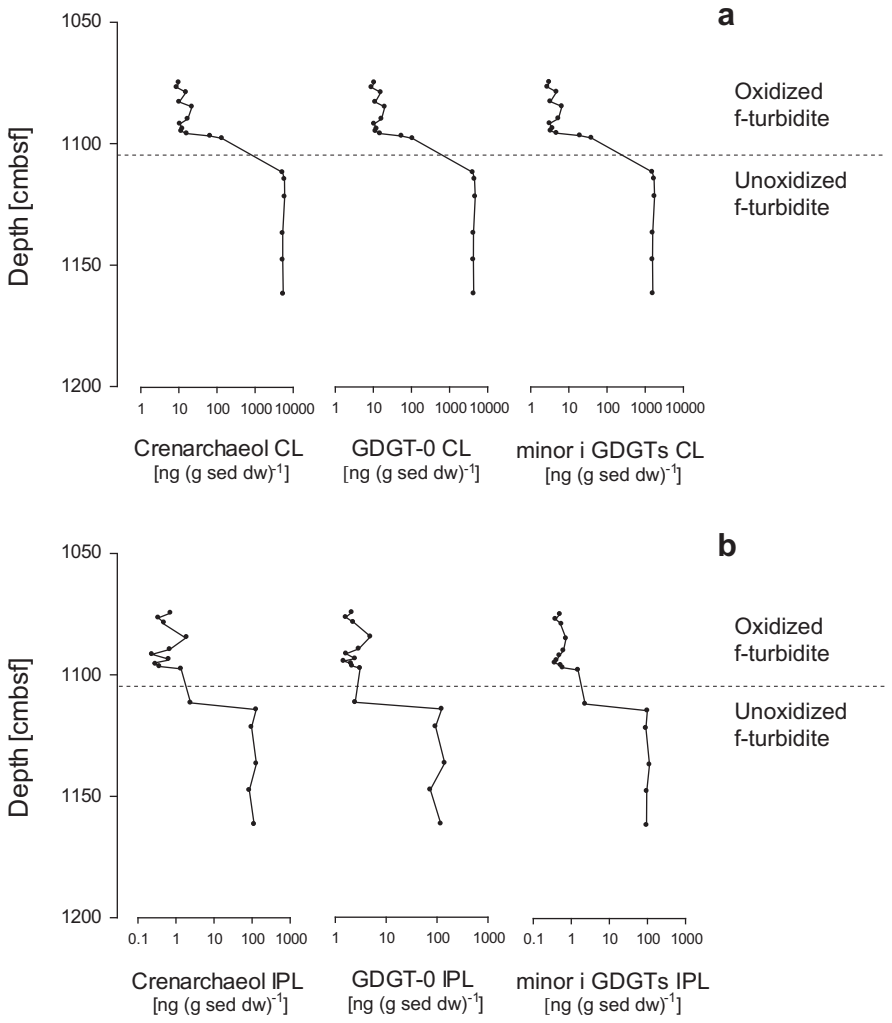

Fig. 4. Lipid concentrations in the f-turbidite. Concentrations [ng (g sed dw^{-1})] of CL (a) and IPL-derived (b) lipids for crenarchaeol, GDGT-0, and the sum of the minor iGDGTs (GDGT-1, -2, -3 and crenarchaeol region isomer) in the f-turbidite. Note log scale.

here, i.e. in situ production of a small amount of IPL iGDGTs in the oxidized sediment by sedimentary aerobic Thaumarchaeota. These likely function via aerobic oxidation of NH_4^+ (Könneke et al., 2005; Wuchter et al., 2006b; de la Torre et al., 2008; Walker et al., 2010; Tourna et al., 2011), formed from the breakdown of OM when O_2 penetrated the sediments.

To examine the oxic degradation and potential production of individual IPL iGDGTs, we performed direct analysis of IPL crenarchaeol. Analysis of the unoxidized sediment showed the presence of two main intact polar lipid species, MH crenarchaeol and DH crenarchaeol, while no HPH crenarchaeol was detected. The distribution is different from the distribution in cultures, where HPH crenarchaeol is always present (Schouten et al., 2008; Pitcher et al., 2010, 2011b; Sinninghe Damsté et al., 2012) but is similar to that of IPLs in deeper marine sediments (Biddle et al., 2006; Lipp and Hinrichs, 2009). The absence of HPH crenarchaeol is probably due to the greater lability of this IPL GDGT, as shown for Arabian Sea sediments, where degradation at the surface occurred within a few cm (Lengger et al., 2012b). This was also predicted from results of theoretical modeling (Schouten et al., 2010; Xie et al., 2013). As direct quantification was not possible with SRM due to the lack of authentic standards, we used semi-preparative HPLC of a composite sample of the unoxidized sediment to isolate the MH GDGT and DH GDGT fractions and subjected them to hydrolysis, after which the resulting GDGTs were quantified through comparison with an internal standard. The results were then used for indirect quantification of the other turbidite samples (Section 2.6). The MH crenarchaeol and DH crenarchaeol concentration in the unoxidized sediments showed little variation (ca. 80 ng (g sed dw)$^{-1}$ for MH crenarchaeol and ca. 10 ng (g sed dw)$^{-1}$ for DH crenarchaeol) but was substantially lower in the oxidized turbidite (avg. 1.0 and 0.01 ng (g sed dw)$^{-1}$, respectively; Table 2; Fig. 5).

DH crenarchaeol exhibited a lower apparent preservation efficiency than CL crenarchaeol, suggesting it was more labile, as would be expected for an IPL. In contrast, the apparent preservation efficiency of MH crenarchaeol (1.3%) was substantially higher than that of DH crenarchaeol (0.1%) and was also higher than that of CL- derived and IPL-derived crenarchaeol. The reason for the high apparent preservation efficiency of MH crenarchaeol could be greater stability than for DH crenarchaeol and CL crenarchaeol. However, this seems unlikely as functionalized compounds are likely more readily degradable than CL GDGTs. It is also possible that MH crenarchaeol is partially derived from DH crenarchaeol which, if only one hexose group is removed, would produce MH crenarchaeol. Another possibility is that MH crenarchaeol is produced in situ by aerobic Thaumarchaeota, as discussed above. Such production in the oxidized part of the sediment would then lead to a smaller than expected decrease in the amount of MH crenarchaeol. However, it would also imply that these sedimentary Thaumarchaeota would only produce MH crenarchaeol and no substantial amounts of DH and HPH crenarchaeol. This seems unlikely as sedimentary and soil Thaumarchaeota in enrichment cultures (Pitcher et al., 2011b; Sinninghe Damsté

Table 2
Concentration in unoxidized part of turbidite of MH GDGTs and DH GDGTs and their sum, isolated via preparative HPLC, and average of IPL-derived GDGTs isolated via silica column (concentration in ng per g sediment dry wt.).

	GDGT-0	GDGT-1	GDGT-2	GDGT-3	Crenarchaeol	Crenarchaeol regioisomer	Total	TEX_{86}
MH	113	9.7	7.2	1.6	80.9	3.4	216	0.55
DH	18.9	10.7	15.0	3.6	10.0	6.0	64.4	0.70
Sum	132	20.5	22.2	5.2	91.0	9.3	280	0.64
IPL-derived	110	34	40	9.6	111	15	320	0.66

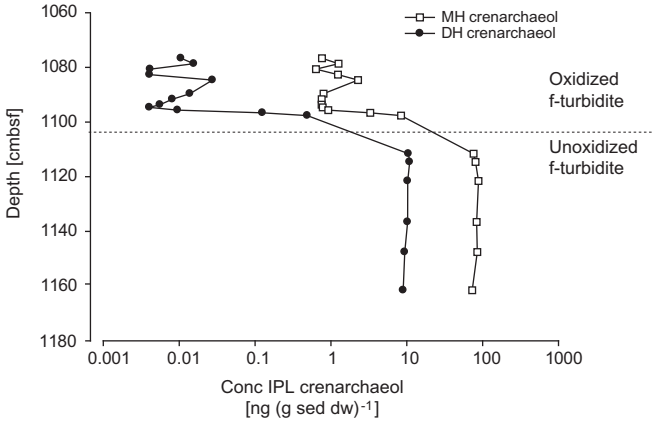

Fig. 5. Concentration [ng (g sed dw)$^{-1}$] of MH and DH crenarchaeol. Note log scale.

et al., 2012) and in surface sediments (Lengger et al., 2012b) do synthesize GDGTs with MH, DH and HPH head groups. Alternatively, part of the MH crenarchaeol and, to a minor extent, DH crenarchaeol, could also stem from a terrigenous source, resulting in enhanced preservation, as discussed above for the brGDGTs. If so, soil Thaumarchaeota would produce more MH crenarchaeol than DH crenarchaeol, in contrast to results reported from enrichment cultures (Sinninghe Damsté et al., 2012) and to reports of the presence of MH, DH and HPH crenarchaeol in riverine suspended particulate matter (SPM) from the River Amazon (Zell et al., 2013). Nevertheless, there has been no quantitative detailed survey of IPL GDGTs in terrigenous OM or riverine SPM, so it is difficult to evaluate this hypothesis. Thus, a combination of in situ produced IPL GDGTs and preferential degradation of marine vs. terrestrial OM may be the cause of the apparent enhanced preservation of MH crenarchaeol in the oxidized part of the sediment.

3.4. Effect of post-depositional oxidation on MBT/CBT, BIT index and TEX_{86} proxies

As stated above, the MBT/CBT proxy is affected by post-depositional oxidation and values change for the CL GDGTs to, presumably, more terrigenous values (Fig. 3g). The BIT index increased strongly with increasing level of oxygen exposure, from an average of 0.01 for the CLs in the non-oxidized section to 0.2 in the oxidized section and from 0.1 in the non-oxidized sediment to as high as 0.5 for the IPL-derived GDGTs in the oxidized part (Fig. 6a and b). The results for the core lipids agree with those reported by Huguet et al. (2008). Over the oxidized section, a gradual increase in BIT index was observed, associated with the decrease in concentration, indicating that the increase in BIT only occurs upon substantial degradation. Intriguingly, the effect is stronger for the IPL-derived BIT (increase by 0.6 units) than for the CL- derived BIT (increase by 0.3 units). The higher BIT value for IPL-derived GDGTs could be due to either enhanced preservation of brGDGTs over crenarchaeol, or to enhanced in situ production of brGDGTs over iGDGTs in the oxidized part of the turbidite, as discussed above.

TEX_{86} values for the CL GDGTs showed hardly any change upon oxidation, despite the large drop in concentration of CL iGDGTs (Fig. 6c), and were always lower than the TEX_{86} values for the IPL iGDGTs (0.53; Fig. 6d). This partially agrees with the results obtained by Huguet et al. (2009), who observed an increase in TEX_{86} in the f-turbidite upon oxidation, but not for all the other turbidite deposits examined (ibid.). In contrast to the CL fraction, TEX_{86} for the IPL-derived fraction decreased strongly upon oxidation, by ca. 0.07 from 0.64 to 0.57. Apart from in situ production, another reason why TEX_{86} for IPL-derived GDGTs changed could be the observed apparent preservation of the MH GDGTs vs. the DH GDGTs, as discussed above (Fig. 5). It has been shown that the ring distribution, and thus TEX_{86} from IPLs, varies with head group in thaumarchaeal cultures and marine sediments (Sinninghe Damsté et al., 2012; Lengger et al., 2012b). In order to examine the impact differential degradation could have on TEX_{86}, MH GDGT and DH GDGT fractions were isolated via semi-preparative HPLC from a combined sample of the unoxidized f-turbidite. Other IPLs might have been present in minor amounts in the IPL fraction, but the similarity of the summed amount of MH and DH crenarchaeol in the unoxidized sediment [90 ng (g sed dw)$^{-1}$] to the average amount of IPL crenarchaeol in the unoxidized sediment [110 ng (g sed dw)$^{-1}$] suggested that they represented the main IPL GDGTs. The TEX_{86} value was 0.55 for the MH GDGTs and 0.70 for the DH GDGTs (Table 2), with a weighted average value of 0.64. This is consistent with results from thaumarchaeal cultures, which showed that MH GDGTs and HPH GDGTs had a greater contribution from GDGT-1, while DH GDGTs consisted mainly of GDGT-2, -3 and -4 (Schouten et al., 2008; Pitcher et al., 2011b; Sinninghe Damsté et al., 2012). Considering the substantial differences between TEX_{86} values from MH GDGTs and DH GDGTs (0.15), the proportional decrease in DH GDGTs vs. MH GDGTs in the oxidized part of the turbidite (Figs. 5 and 6), should result in a shift in TEX_{86}.

To test our hypothesis, we calculated the theoretical TEX_{86} values based on the concentration of MH-derived and DH-derived GDGTs, measured using preparative HPLC, for the unoxidized turbidite ($GDGT_{MH}$ and $GDGT_{DH}$, respectively) and the proportion of MH crenarchaeol vs. the sum of MH crenarchaeol and DH crenarchaeol, f_{MH}, as determined from SRM measurements:

$$TEX_{86,theor} = \frac{(GDGT-2_{MH} + GDGT\text{-}3_{MH} + Cren'_{MH}) * f_{MH} + (GDGT\text{-}2_{DH} + GDGT\text{-}3_{DH} + Cren'_{DH}) * (1 - f_{MH})}{(GDGT\text{-}1_{MH} + GDGT\text{-}2_{MH} + GDGT\text{-}3_{MH} + Cren'_{MH}) * f_{MH} + (GDGT\text{-}1_{DH} + GDGT\text{-}2_{DH} + GDGT\text{-}3_{DH} + Cren'_{DH}) * (1 - f_{MH})} \quad (1)$$

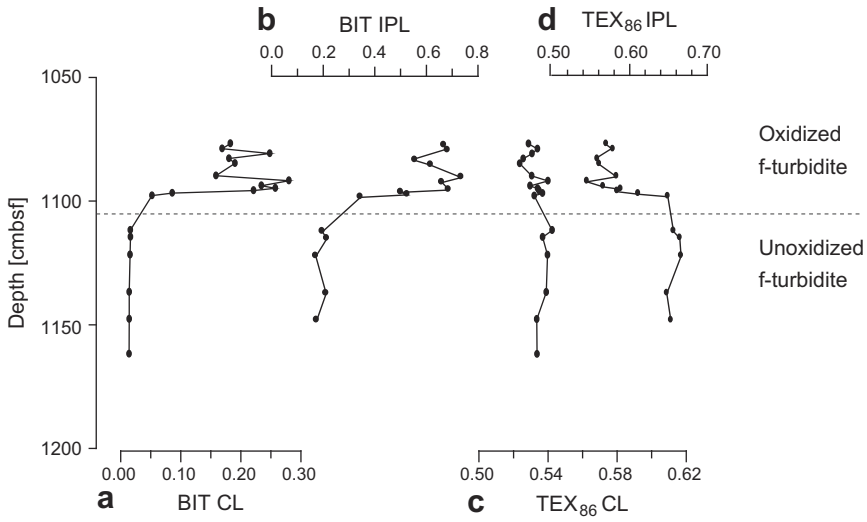

Fig. 6. CL- and IPL-derived BIT (a, b) and TEX_{86} (c, d) values from f-turbidite in oxidized and unoxidized part.

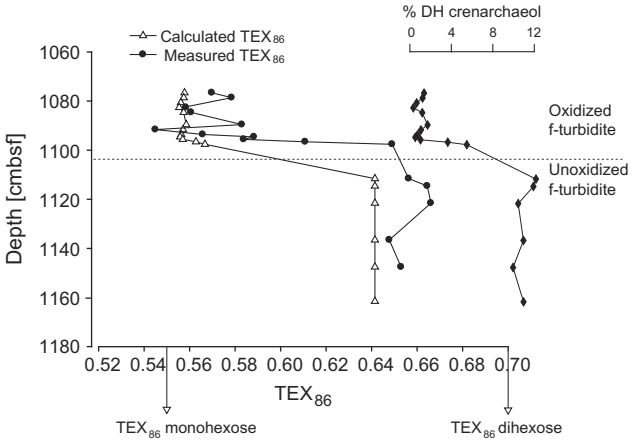

Fig. 7. TEX_{86} values calculated from relative proportions of MH GDGTs and DH GDGTs vs. measured TEX_{86} values for IPL-derived GDGTs, acc. to Eq. (1); and proportion of DH crenarchaeol of total (MH + DH) IPL-derived crenarchaeol.

Using Eq. (1), a decrease in TEX_{86} from 0.64 to 0.56–0.57 upon oxidation was predicted due to the changing proportion of MH GDGTs vs. DH GDGTs (Fig. 7), which was similar to the measured IPL-derived TEX_{86} values (Fig. 5; Table 2). Thus, the change in IPL-derived TEX_{86} could be due to the greater apparent preservation efficiency of MH GDGTs vs. DH GDGTs.

Apparently, the degradation and in situ production of IPL GDGTs has no influence on TEX_{86} from CL GDGTs. This suggests that IPL GDGTs potentially produced in situ are degraded completely and do not accumulate as CL GDGTs. Furthermore, the amount of IPL iGDGTs is small vs. the respective CL iGDGTs (3–6% in the unoxidized sediment; Table 1). It is thus likely that the IPL GDGTs are present in too small an amount to significantly influence TEX_{86} for CL iGDGTs, which is the value ultimately used for paleotemperature estimation.

4. Conclusions

Both CL and IPL GDGTs were strongly degraded upon post-depositional oxidation of the organic-rich f-turbidite from the Madeira Abyssal Plain. Degradation patterns revealed that terrestrial GDGTs were relatively better preserved, while marine GDGTs seemed to be relatively more labile, resulting in changes in the BIT index upon oxidation, in line with previous studies. Surprisingly, some IPL GDGTs appeared to be better preserved upon oxidation than CL GDGTs. Similarly, the directly measured IPL MH crenarchaeol, was apparently preserved better than CL crenarchaeol. This apparent preservation of some IPL GDGTs is likely due to a combination of enhanced preservation of terrigenous vs. marine GDGTs as well as some minor in situ production. Since MH GDGTs showed lower TEX_{86} values than DH GDGTs, the apparent preferential preservation resulted in changes in TEX_{86} for the IPL-derived GDGTs. However, the TEX_{86} from CL GDGTs, ultimately used in paleotemperature estimation, was not affected by post-depositional oxidation, most likely due to the small amount of IPL GDGTs vs. CL GDGTs (< 10%). Contrastingly, there was a large change in BIT values upon oxidation, as well as in MBT/CBT, suggesting that care has to be taken with the interpretation of proxies containing brGDGTs, when they are present in low amount and have been exposed to post-depositional oxidation. Furthermore, our results show that progressive degradation can cause changes in abundance and distribution of IPL GDGTs in sediments due to a combination of in situ production and preferential preservation of terrestrial sourced GDGTs.

Acknowledgements

The authors would like to thank the participants in the JCR209 and the Master and crew of the R/V James Clark Ross, as well as two anonymous reviewers for constructive comments. Thanked for analytical assistance are R. Gieles, J. Ossebaar and F. Temmesfeld. S.K.L. was funded partially by a grant from the Darwin Center for Biogeosciences to S.S. This is publication number DW-2013-1006 of the Darwin Center for Biogeosciences.

Associate Editor—**K.-U. Hinrichs**

References

Aitchison, J., 1981. A new approach to null correlations of proportions. Journal of the International Association for Mathematical Geology 13, 175–189.

Albers, S.-V., Meyer, B.H., 2011. The archaeal cell envelope. Nature Reviews Microbiology 9, 414–427.

Biddle, J.F., Lipp, J.S., Lever, M.A., Lloyd, K.G., Sørensen, K.B., Anderson, R., Fredricks, H.F., Elvert, M., Kelly, T.J., Schrag, D.P., Sogin, M.L., Brenchley, J.E., Teske, A., House, C.H., Hinrichs, K.-U., 2006. Heterotrophic Archaea dominate sedimentary subsurface ecosystems off Peru. Proceedings of the National Academy of Sciences of the United States of America 103, 3846–3851.

Bligh, E.G., Dyer, W.J., 1959. A rapid method of total lipid extraction and purification. Canadian Journal of Biochemistry and Physiology 37, 911–917.
Bloemsma, M.R., Zabel, M., Stuut, J.B.W., Tjallingii, R., Collins, J.A., Weltje, G.J., 2012. Modelling the joint variability of grain size and chemical composition in sediments. Sedimentary Geology 280, 135–148.
Bouma, A.H., 1962. Sedimentology of Some Flysch Deposits: A Graphic Approach to Facies Interpretation. Elsevier Pub. Co., Amsterdam, New York.
Brochier-Armanet, C., Boussau, B., Gribaldo, S., Forterre, P., 2008. Mesophilic crenarchaeota: proposal for a third archaeal phylum, the Thaumarchaeota. Nature Reviews Microbiology 6, 245–252.
Buckley, D.E., Cranston, R.E., 1988. Early diagenesis in deep sea turbidites: the imprint of paleo-oxidation zones. Geochimica et Cosmochimica Acta 52, 2925–2939.
Cowie, G., Calvert, S., de Lange, G., Keil, R., Hedges, J., 1998. Extents and implications of organic matter alteration at oxidation fronts in turbidites from the Madeira Abyssal Plain. In: Proceedings of the Ocean Drilling Program, Scientific Results Leg 157. US Government Printing Office, Washington, DC, pp. 581–589.
Cowie, G.L., Hedges, J.I., Prahl, F.G., de Lange, G.J., 1995. Elemental and major biochemical changes across an oxidation front in a relict turbidite: An oxygen effect. Geochimica et Cosmochimica Acta 59, 33–46.
de la Torre, J.R., Walker, C.B., Ingalls, A.E., Könneke, M., Stahl, D.A., 2008. Cultivation of a thermophilic ammonia oxidizing archaeon synthesizing crenarchaeol. Environmental Microbiology 10, 810–818.
De Lange, G.J., 1992. Distribution of exchangeable, fixed, organic and total nitrogen in interbedded turbiditic/pelagic sediments of the Madeira Abyssal Plain, eastern North Atlantic. Marine Geology 109, 95–114.
Harvey, H.R., Fallon, R.D., Patton, J.S., 1986. The effect of organic matter and oxygen on the degradation of bacterial membrane lipids in marine sediments. Geochimica et Cosmochimica Acta 50, 795–804.
Hoefs, M.J.L., Rijpstra, W.I.C., Sinninghe Damsté, J.S., 2002. The influence of oxic degradation on the sedimentary biomarker record I: Evidence from Madeira Abyssal Plain turbidites. Geochimica et Cosmochimica Acta 66, 2719–2735.
Hopmans, E.C., Weijers, J.W.H., Schefuß, E., Herfort, L., Sinninghe Damsté, J.S., Schouten, S., 2004. A novel proxy for terrestrial organic matter in sediments based on branched and isoprenoid tetraether lipids. Earth and Planetary Science Letters 224, 107–116.
Huguet, C., Hopmans, E.C., Febo-Ayala, W., Thompson, D.H., Sinninghe Damsté, J.S., Schouten, S., 2006. An improved method to determine the absolute abundance of glycerol dibiphytanyl glycerol tetraether lipids. Organic Geochemistry 37, 1036–1041.
Huguet, C., de Lange, G.J., Gustafsson, Ö., Middelburg, J.J., Sinninghe Damsté, J.S., Schouten, S., 2008. Selective preservation of soil organic matter in oxidized marine sediments (Madeira Abyssal Plain). Geochimica et Cosmochimica Acta 72, 6061–6068.
Huguet, C., Kim, J.-H., de Lange, G.J., Sinninghe Damsté, J.S., Schouten, S., 2009. Effects of long term oxic degradation on the $U^{K'}_{37}$, TEX_{86} and BIT organic proxies. Organic Geochemistry 40, 1188–1194.
Jenkyns, H.C., Schouten-Huibers, L., Schouten, S., Sinninghe Damsté, J.S., 2012. Warm Middle Jurassic-Early Cretaceous high-latitude sea-surface temperature from the Southern Ocean. Climate of the Past 8, 215–226.
Keil, R.G., Montluçon, D.B., Prahl, F.G., Hedges, J.I., 1994. Sorptive preservation of labile organic matter in marine-sediments. Nature 370, 549–552.
Kim, J.-H., Schouten, S., Hopmans, E.C., Donner, B., Sinninghe Damsté, J.S., 2008. Global sediment core-top calibration of the TEX_{86} paleothermometer in the ocean. Geochimica et Cosmochimica Acta 72, 1154–1173.
Kim, J.-H., Huguet, C., Zonneveld, K.A.F., Versteegh, G.J.M., Roeder, W., Sinninghe Damsté, J.S., Schouten, S., 2009. An experimental field study to test the stability of lipids used for the TEX_{86} and $U^{K'}_{37}$ palaeothermometers. Geochimica et Cosmochimica Acta 73, 2888–2898.
Kim, J.-H., van der Meer, J., Schouten, S., Helmke, P., Willmott, V., Sangiorgi, F., Koç, N., Hopmans, E.C., Sinninghe Damsté, J.S., 2010. New indices and calibrations derived from the distribution of crenarchaeal isoprenoid tetraether lipids: implications for past sea surface temperature reconstructions. Geochimica et Cosmochimica Acta 74, 4639–4654.
Koga, Y., Morii, H., 2005. Recent advances in structural research on ether lipids from archaea including comparative and physiological aspects. Bioscience Biotechnology and Biochemistry 69, 2019–2034.
Könneke, M., Bernhard, A.E., de la Torre, J.R., Walker, C.B., Waterbury, J.B., Stahl, D.A., 2005. Isolation of an autotrophic ammonia-oxidizing marine archaeon. Nature 437, 543–546.
Kuypers, M.M.M., Blokker, P., Erbacher, J., Kinkel, H., Pancost, R.D., Schouten, S., Sinninghe Damsté, J.S., 2001. Massive expansion of marine archaea during a mid-cretaceous oceanic anoxic event. Science 293, 92–94.
Lengger, S.K., Hopmans, E.C., Sinninghe Damsté, J.S., Schouten, S., 2012a. Comparison of extraction and work up techniques for analysis of core and intact polar tetraether lipids from sedimentary environments. Organic Geochemistry 47, 34–40.
Lengger, S.K., Hopmans, E.C., Reichart, G.-J., Nierop, K.G.J., Sinninghe Damsté, J.S., Schouten, S., 2012b. Intact polar and core glycerol dibiphytanyl glycerol tetraether lipids in the Arabian Sea oxygen minimum zone: II. Selective preservation and degradation in sediments and consequences for the TEX_{86}. Geochimica et Cosmochimica Acta 98, 244–258.
Lin, Y.S., Lipp, J.S., Elvert, M., Holler, T., Hinrichs, K.-U., 2012. Assessing production of the ubiquitous archaeal diglycosyl tetraether lipids in marine subsurface sediment using intramolecular stable isotope probing. Environmental Microbiology.
Lipp, J.S., Morono, Y., Inagaki, F., Hinrichs, K.-U., 2008. Significant contribution of Archaea to extant biomass in marine subsurface sediments. Nature 454, 991–994.
Lipp, J.S., Hinrichs, K.-U., 2009. Structural diversity and fate of intact polar lipids in marine sediments. Geochimica et Cosmochimica Acta 73, 6816–6833.
Liu, X., Lipp, J.S., Hinrichs, K.-U., 2011. Distribution of intact and core GDGTs in marine sediments. Organic Geochemistry 42, 368–375.
Logemann, J., Graue, J., Köster, J., Engelen, B., Rullkötter, J., Cypionka, H., 2011. A laboratory experiment of intact polar lipid degradation in sandy sediments. Biogeosciences 8, 2547–2560.
McGregor, H.V., Dupont, l., Stuut, J.-B.W., Kuhlmann, H., 2009. Vegetation change, goats, and religion: a 2000-year history of land use in southern Morocco. Quaternary Science Reviews 28, 1434–1448.
Middelburg, J.J., 1989. A simple rate model for organic matter decomposition in marine sediments. Geochimica et Cosmochimica Acta 53, 1577–1581.
Peterse, F., Kim, J.-H., Schouten, S., Klitgaard Kristensen, D., Koç, N., Sinninghe Damsté, J.S., 2009. Constraints on the application of the MBT/CBT palaeothermometer at high latitude environments (Svalbard, Norway). Organic Geochemistry 40, 692–699.
Peterse, F., Hopmans, E.C., Schouten, S., Mets, A., Rijpstra, W.I.C., Sinninghe Damsté, J.S., 2011. Identification and distribution of intact polar branched tetraether lipids in peat and soils. Organic Geochemistry 42, 1007–1015.
Peterse, F., van der Meer, J., Schouten, S., Weijers, J.W.H., Fierer, N., Jackson, R.B., Kim, J.-H., Sinninghe Damsté, J.S., 2012. Revised calibration of the MBT-CBT paleotemperature proxy based on branched tetraether membrane lipids in surface soils. Geochimica et Cosmochimica Acta 96, 215–229.
Pitcher, A., Hopmans, E.C., Schouten, S., Sinninghe Damsté, J.S., 2009. Separation of core and intact polar archaeal tetraether lipids using silica columns: Insights into living and fossil biomass contributions. Organic Geochemistry 40, 12–19.
Pitcher, A., Rychlik, N., Hopmans, E.C., Spieck, E., Rijpstra, W.I.C., Ossebaar, J., Schouten, S., Wagner, M., Sinninghe Damsté, J.S., 2010. Crenarchaeol dominates the membrane lipids of *Candidatus* Nitrososphaera gargensis, a thermophilic Group I.1b Archaeon. International Society for Microbial Ecology 4, 542–552.
Pitcher, A., Hopmans, E.C., Villanueva, L., Reichart, G.-J., Schouten, S., Sinninghe Damsté, J.S., 2011a. Niche segregation of Ammonia-oxidizing Archaea and Anammox bacteria in the Arabian Sea oxygen minimum zone. ISME Journal 5, 1896–1904.
Pitcher, A., Hopmans, E.C., Mosier, A.C., Park, S.-J., Rhee, S.-K., Francis, C.A., Schouten, S., Sinninghe Damsté, J.S., 2011b. Core and intact polar glycerol dibiphytanyl glycerol tetraether lipids of ammonia-oxidizing archaea enriched from marine and estuarine sediments. Applied and Environmental Microbiology 77, 3468–3477.
Prahl, F.G., de Lange, G.J., Scholten, S., Cowie, G.L., 1997. A case of post-depositional aerobic degradation of terrestrial organic matter in turbidite deposits from the Madeira Abyssal Plain. Organic Geochemistry 27, 141–152.
Schouten, S., Hopmans, E.C., Schefuß, E., Sinninghe Damsté, J.S., 2002. Distributional variations in marine crenarchaeotal membrane lipids: a new tool for reconstructing ancient sea water temperatures? Earth and Planetary Science Letters 204, 265–274.
Schouten, S., Hopmans, E.C., Sinninghe Damsté, J.S., 2004. The effect of maturity and depositional redox conditions on archaeal tetraether lipid palaeothermometry. Organic Geochemistry 35, 567–571.
Schouten, S., Huguet, C., Hopmans, E.C., Kienhuis, M.V.M., Sinninghe Damsté, J.S., 2007. Analytical methodology for TEX_{86} paleothermometry by high-performance liquid chromatography/atmospheric pressure chemical ionization-mass spectrometry. Analytical Chemistry 79, 2940–2944.
Schouten, S., Hopmans, E.C., Baas, M., Boumann, H., Standfest, S., Könneke, M., Stahl, D.A., Sinninghe Damsté, J.S., 2008. Intact membrane lipids of "Candidatus Nitrosopumilus maritimus", a cultivated representative of the cosmopolitan mesophilic group I crenarchaeota. Applied and Environmental Microbiology 74, 2433–2440.
Schouten, S., Middelburg, J.J., Hopmans, E.C., Sinninghe Damsté, J.S., 2010. Fossilization and degradation of intact polar lipids in deep subsurface sediments: a theoretical approach. Geochimica et Cosmochimica Acta 74, 3806–3814.
Schouten, S., Hopmans, E.C., Sinninghe Damsté, J.S., 2013. The organic geochemistry of glycerol dialkyl glycerol tetraether lipids: A review. Organic Geochemistry 54, 19–61.
Schubotz, F., Wakeham, S.G., Lipp, J.S., Fredricks, H.F., Hinrichs, K.-U., 2009. Detection of microbial biomass by intact polar membrane lipid analysis in the water column and surface sediments of the Black Sea. Environmental Microbiology 11, 2720–2734.
Sinninghe Damsté, J.S., Rijpstra, W.I.C., Reichart, G.-J., 2002. The influence of oxic degradation on the sedimentary biomarker record II. Evidence from Arabian Sea sediments. Geochimica et Cosmochimica Acta 66, 2737–2754.
Sinninghe Damsté, J.S., Rijpstra, W.I.C., Hopmans, E.C., Jung, M.Y., Kim, J.G., Rhee, S.K., Stieglmeier, M., Schleper, C., 2012. Intact polar and core dibiphytanyl glycerol tetraether lipids of group I. 1a and I. 1b Thaumarchaeota in soil. Applied and Environmental Microbiology 78, 6866–6874.
Smith, R.W., Bianchi, T.S., Li, X., 2012. A re-evaluation of the use of branched GDGTs as terrestrial biomarkers: implications for the BIT Index. Geochimica et Cosmochimica Acta 80, 14–29.
Spang, A., Hatzenpichler, R., Brochier-Armanet, C., Rattei, T., Tischler, P., Spieck, E., Streit, W., Stahl, D.A., Wagner, M., Schleper, C., 2010. Distinct gene set in two

different lineages of ammonia-oxidizing archaea supports the phylum Thaumarchaeota. Trends in Microbiology 18, 331–340.
Sturt, H.F., Summons, R.E., Smith, K., Elvert, M., Hinrichs, K.-U., 2004. Intact polar membrane lipids in prokaryotes and sediments deciphered by high-performance liquid chromatography/electrospray ionization multistage mass spectrometry – new biomarkers for biogeochemistry and microbial ecology. Rapid Communications in Mass Spectrometry 18, 617–628.
Takano, Y., Chikaraishi, Y., Ogawa, N.O., Nomaki, H., Morono, Y., Inagaki, F., Kitazato, H., Hinrichs, K.-U., Ohkouchi, N., 2010. Sedimentary membrane lipids recycled by deep-sea benthic archaea. Nature Geoscience 3, 858–861.
Tjallingii, R., Röhl, U., Kölling, M., Bickert, T., 2007. Influence on the water content on X-ray fluorescence core-scanning measurements in soft marine sediments. Geochemistry Geophysics Geosystems 8, Q02004.
Tourna, M., Stieglmeier, M., Spang, A., Könneke, M., Schintlmeister, A., Urich, T., Engel, M., Schloter, M., Wagner, M., Richter, A., Schleper, C., 2011. Nitrososphaera viennensis, an ammonia oxidizing archaeon from soil. Proceedings of the National Academy of Sciences of the United States of America 108, 8420–8425.
Walker, C.B., de la Torre, J.R., Klotz, M.G., Urakawa, H., Pinel, N., Arp, D.J., Brochier-Armanet, C., Chain, P.S.G., Chan, P.P., Gollabgir, A., Hemp, J., Hügler, M., Könneke, M., Shin, M., Lawton, T.J., Lowe, T., Martens-Habbena, W., Sayavedra-Soto, L.A., Lang, D., Sievert, S.M., Rosenzweig, A.C., Manning, G., Stahl, D.A., 2010. Nitrosopumilus maritimus genome reveals unique mechanisms for nitrification and autotrophy in globally distributed marine crenarchaea. Proceedings of the National Academy of Sciences of the United States of America 107, 8818–8823.
Weaver, P.P.E., Kuijpers, A., 1983. Climatic control of turbidite deposition during the last 200,000 years on the Madeira Abyssal Plain. Nature 306, 360–363.
Weaver, P.P.E., Buckley, D.E., Kuijpers, A., 1989. Geological investigations of ESOPE cores from the Madeira Abyssal Plain. In: Geoscience Investigations of Two North Atlantic Abyssal Plains – The ESOPE International Expedition. OECD/NEA-Seabed Working group. Commission of European Communities Joint Research Centre, Ispra, pp. 535–555.
Weijers, J.W.H., Schouten, S., van den Donker, J.C., Hopmans, E.C., Sinninghe Damsté, J.S., 2007. Environmental controls on bacterial tetraether membrane lipid distribution in soils. Geochimica et Cosmochimica Acta 71, 703–713.
Weijers, J.W.H., Panoto, E., van Bleijswijk, J., Schouten, S., Rijpstra, W.I.C., Balk, M., Stams, A.J.M., Sinninghe Damsté, J.S., 2009. Constraints on the biological source(s) of the orphan branched tetraether membrane lipids. Geomicrobiology Journal 26, 402–414.
Weltje, G.J., Tjallingii, R., 2008. Calibration of XRF core scanners for quantitative geochemical logging of sediment cores: theory and application. Earth and Planetary Science Letters 274, 423–438.
White, D.C., Davis, W.M., Nickels, J.S., King, J.D., Bobbie, R.J., 1979. Determination of the sedimentary microbial biomass by extractible lipid phosphate. Oecologia 40, 51–62.
Wuchter, C., Schouten, S., Wakeham, S.G., Sinninghe Damsté, J.S., 2005. Temporal and spatial variation in tetraether membrane lipids of marine Crenarchaeota in particulate organic matter: implications for TEX_{86} paleothermometry. Paleoceanography 20, PA3013.
Wuchter, C., Schouten, S., Wakeham, S.G., Sinninghe Damsté, J.S., 2006a. Archaeal tetraether membrane lipid fluxes in the northeastern Pacific and the Arabian Sea: implications for TEX_{86} paleothermometry. Paleoceanography 21, PA4208.
Wuchter, C., Abbas, B., Coolen, M.J.L., Herfort, L., van Bleijswijk, J., Timmers, P., Strous, M., Teira, E., Herndl, G.J., Middelburg, J.J., Schouten, S., Sinninghe Damsté, J.S., 2006b. Archaeal nitrification in the ocean. Proceedings of the National Academy of Sciences of the United States of America 103, 12317–12322.
Xie, S., Lipp, J.S., Wegener, G., Ferdelman, T.G., Hinrichs, K.-U., 2013. Turnover of microbial lipids in the deep biosphere and growth of benthic archaeal populations. Proceedings of the National Academy of Sciences of the United States of America 110, 6010–6014.
Zell, C., Kim, J.-H., Moreira-Turcq, P., Abril, G., Hopmans, E.C., Bonnet, M.-P., Lima Sobrinho, R., Sinninghe Damsté, J.S., 2013. Disentangling the origins of branched tetraether lipids and crenarchaeol in the lower Amazon River: implications for GDGT-based proxies. Limnology and Oceanography 58, 343–353.
Zhu, C., Weijers, J.W.H., Wagner, T., Pan, J.-M., Chen, J.-F., Pancost, R.D., 2011. Sources and distributions of tetraetherlipids in surface sediments across a large river-dominated continental margin. Organic Geochemistry 42, 376–386.